Proceedings of the 12th International Conference on
Aluminium Alloys, September 5-9, 2010, Yokohama, Japan

pp. 1291-1295

Direct Observation of Solidification Behavior in Al-Si-Cu-Fe System

Bonghwan Kim[1], Hideyuki Yasuda[2] and Sangmok Lee[1]

[1]Liquid Processing & Casting Technology R/D Department, Korea Institute of Industrial Technology, 7-47 Songdo-dong, Yeonsu-gu, Incheon, Korea

[2]Department of adaptive Machine Systems, Osaka University, 2-1 Yamada-oka, Suita, Osaka, Japan

The solidification behaviors of intermetallic phases in low/high levels of iron containing Al-Si-Cu alloys were studied by time-resolved observation technique using synchrotron radiation. In the low iron-containing alloy, the formation of eutectic β-Al_5FeSi phase was clearly recorded after dendritic α-Al growth. On the other hand, in the high iron-containing alloy, not only pseudo-peritectic but also aggregation behavior between the α-AlFeSi and β-Al_5FeSi phases were observed during solidification.

Keywords: *Solidification, Modification, Intermetallic, Al-Si casting alloy, Synchrotron radiation*

1. Introduction

Modification of harmful iron-containing intermetallic phases in the Al-Si casting alloys has been studied as a major topic in aluminum casting industry, especially for the improvement of recycling efficiency of iron rich Al scraps [1]. During the past two decades, representative morphologies of modified iron-containing intermetallic phases by alloying elements such as Mn, Cr, Be, Li, and K etc. have been reported [2-4]. However, the exact stages of solidifications and reactions were not clearly able to understand due to the lack of practical methods to observe the solidification sequences during practical cooling stage.

In the present study, the solidification behaviors of iron-containing intermetallic phases in the Al-Si casting alloys were observed by time-resolved radiography of synchrotron radiation. The iron-rich Al-Si scraps were melted and solidified under a controlled condition in a specially designed vacuum furnace in the storage ring of synchrotron radiation facility. Successive radiograph images were simultaneously obtained by time-resolved methodology during entire stage of solidification. These images were successfully processed by a self-made software to reveal the contrast of relevant phase, eliminating back ground noise in order to compare the formation behaviors of iron-containing intermetallic phases.

2. Experimental procedure

Two kinds of cutting chip scraps of automotive aluminum components were prepared as raw materials in order to study the formation of iron containing intermetallic phases. The ingot materials of each scrap were fabricated by gravity casting process into a Y-block shape permanent mold. The specimens for the real-time observation were prepared by machining and polishing the ingots into the size of 100x100mm of area and 100μm of thickness. The chemical compositions of the specimens were analyzed by inductively coupled plasma-emission spectrometry as summarized in Table 1.

Table 1 Chemical compositions of the iron-containing alloys

Alloy	Chemical composition (wt.%)				
	Si	Cu	Fe	Mn	Al
No. 1 (Low Fe content)	9.5	3.0	1.16	0.14	Bal.
No. 2 (High Fe content)	9.6	2.9	4.19	0.15	Bal.

The specimens were re-melted and solidified in the specially designed vacuum chamber exposed to synchrotron radiation as shown in Fig. 1. The cooling rate was controlled by pulling speed of the heating element around the specimen at 1,000μm/s in an upward direction. The image detector of 0.5μm/pixel resolution was utilized to obtain the series of images during solidification. The obtained series of radiography were processed by a self-made software in order to enhance the contrast of phases and eliminate background noise.

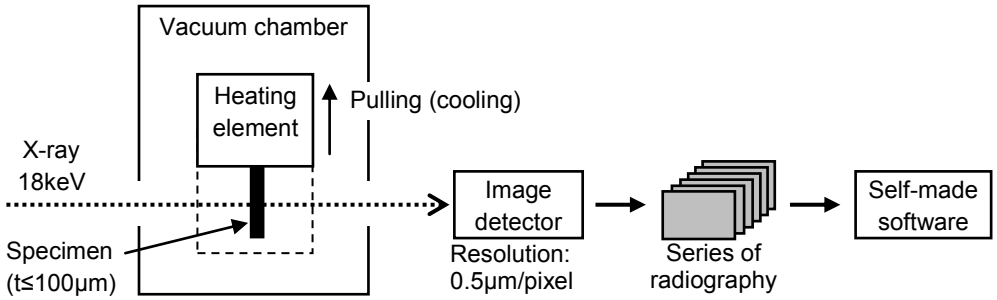

Fig. 1 Block diagram of image processing route based on in-situ solidification experiments in a synchrotron radiation facility.

3. Results and Discussion

The successive radiography of No. 1 alloy in Fig. 2 shows the solidification sequence and the formation behaviors of various intermetallic phases.

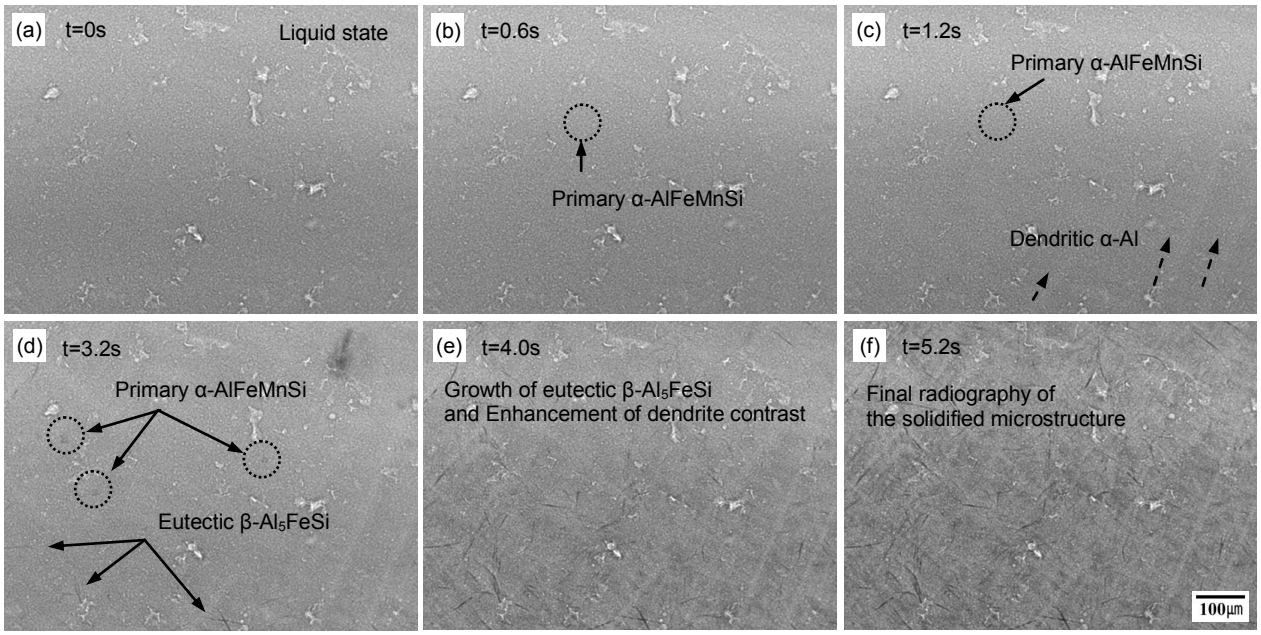

Fig. 2 Successive radiograph images of No. 1 alloy showing solidification sequence.

In the liquid state, small amount of primary α-AlFeMnSi phase started to nucleate and grow just prior to the growth of dendritic α-Al, as shown in Figs. 2(b) and (c). The eutectic β-Al_5FeSi formation was clearly revealed as denoted by arrows at the bottom–left of Fig. 2(d), and the growth of the α-AlFeMnSi phase seemed to be retarded. In the final stage of the solidification, the contrast of radiography was gradually enhanced with the formation progress of eutectic β-Al_5FeSi phase.

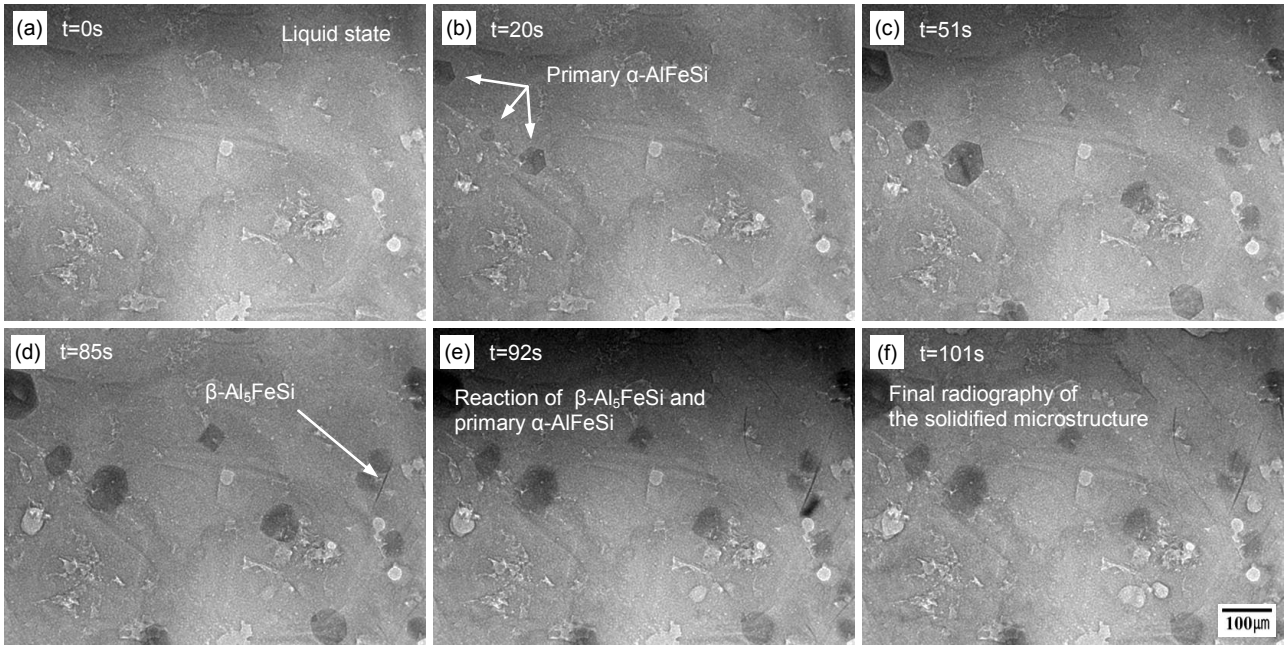

Fig. 3 Successive radiograph images of No. 2 alloy showing solidification sequence.

Dislike to the No. 1 alloy, large amount of equiaxed primary α-AlFeSi phase nucleated and grew with hexagonal morphology in the liquid state as shown in Fig. 3(b). The β-Al_5FeSi phase formed both in the vicinity of the primary α-AlFeSi phase and independently in the liquid as shown in Figs. 3(d) and (e).

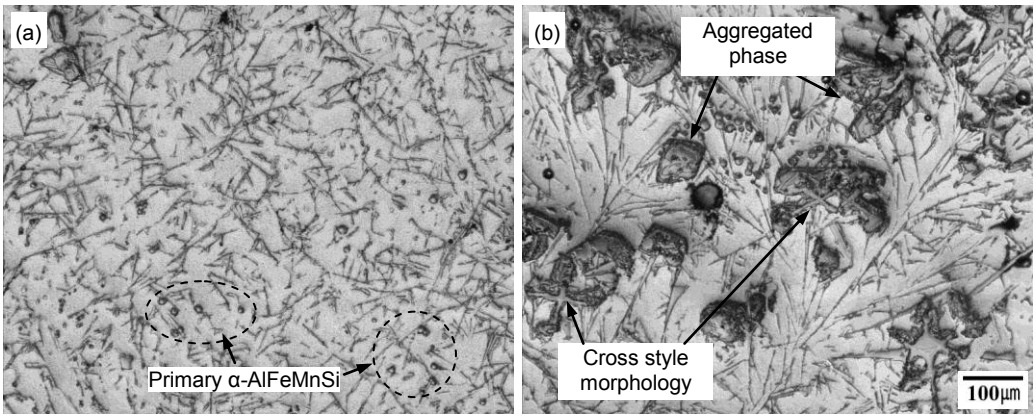

Fig. 4 Typical optical microstructures of (a) No. 1 and (b) No. 2 alloys.

In order to compare with the radiography, optical microstructures of No. 1 and No. 2 alloys were obtained and shown in Figs. 4(a) and (b), respectively. In the microstructure of No. 1 alloy, the constituent phases of α-Al, β-Al_5FeSi, and eutectic Si were confirmed to form the ternary eutectic as major phase. Small equiaxed α-AlFeMnSi phases were also revealed to disperse throughout the specimen. This microstructural evolution was evidently observed in the present radiography (See Fig. 2). In the optical microstructure of No. 2 alloy, two representative morphologies of the α-AlFeSi phase were shown, i.e. cross style and aggregated phase as shown in Fig. 4(b). It is further observed that the cross style phase was mostly connected to the aggregated phase together with the β-Al_5FeSi phase.

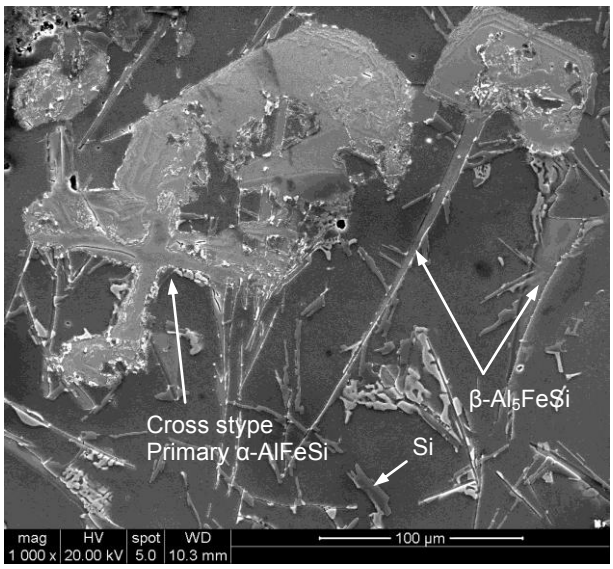

Fig. 5 Scanning electron microscopy of No. 2 alloy showing the representative aggregated forms of various iron-rich intermetallic phases.

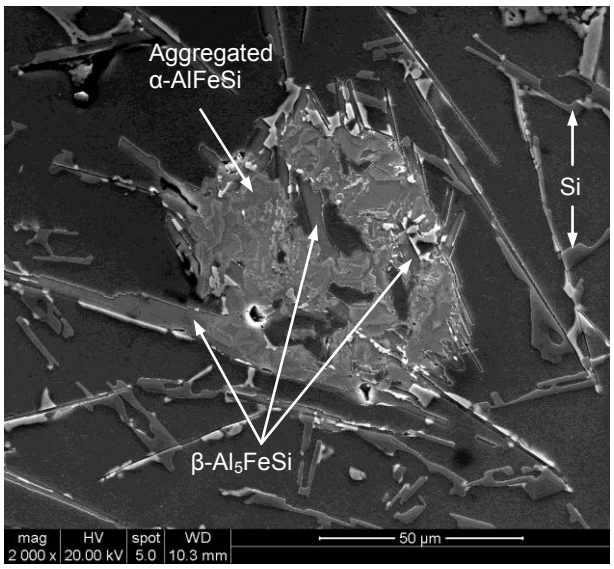

Fig. 6 Scanning electron microscopy of No. 2 alloy showing the pseudo-peritectic reaction between the α-AlFeSi and the needle like β-Al_5FeSi phases.

Fig. 5 shows the scanning electron micrograph (secondary electron image) of No. 2 alloy showing the detailed morphology and the formation behavior of complex shaped phase, consisting of the α-AlFeSi and β-Al_5FeSi phases. Either one or two different morphologies of the primary α-AlFeSi phase, i.e., cross style and aggregated phase were observed to form into further aggregated phase with the β-Al_5FeSi phase as shown in Fig. 5.

Fig. 6 shows the enlarged view of resultant microstructure of pseudo-peritectic reaction processed by the nucleation of the β-Al_5FeSi phase on the aggregated α-AlFeSi substrate. This sequential formation process is clearly demonstrated through Figs. 3(c)-(d). (Note that the needle like β-Al_5FeSi phase was seen to form on the α-AlFeSi phase).

The chemical compositions of the intermetallic phases were checked by EDS analysis for phase identification as summarized in Table 2. Here, chemical compositions were arbitrary measured two times for each specimen for reliability. It is worthwhile to note that the chemical composition of the aggregated α-AlFeSi phase was enriched by minor elements such Cu, Mn, and Cr without noticeable change of major elements, meaning that this phase was formed by incorporating enriched solute atoms at the solidification front which are partitioned at the later stage of solidification. Due to the irregular morphological nature and enriched chemical composition with various minor elements, the aggregated α-AlFeSi phase is regarded as the sludge α-AlFeSi phase. Further work is necessary to confirm this phase more precisely. The sludge α-AlFeSi phase was observed to form either in the vicinity of the cross style α-AlFeSi phase to incorporate or independently in the liquid. It may be suggested that the sludge α-AlFeSi phase gathers nearby intermetallic phases including β-Al_5FeSi phase to form aggregated phase at the later stage of solidification.

Table 2 Phase identification by EDS analysis

Phase	Morphology	Chemical composition (wt.%)					
		Al	Fe	Si	Cu	Mn	Cr
α-Al_8Fe_2Si	Cross	72.83	16.13	11.04	-	-	-
		72.66	16.15	11.19	-	-	-
	Aggregated	72.06	15.18	10.42	1.03	0.67	0.64
		71.94	14.12	10.23	1.55	1.23	0.93
β-Al_5FeSi	Needle	67.08	14.06	18.86	-	-	-
		67.78	13.99	18.23	-	-	-

4. Conclusion

The detailed solidification sequence and resultant morphology of iron containing Al-Si-Cu alloy with the variation of iron content were investigated by combined analysis of time-resolved direct imaging and conventional OM and SEM. In the low iron containing Al-Si-Cu alloy, small amount of α-AlFeMnSi phase formed in the liquid state as a primary followed by the eutectic formation of the β-Al_5FeSi phase. On the other hand, in the high iron containing Al-Si-Cu alloy, the aggregation behavior among various intermetallic phases were observed as well as the pseudo-peritectic reaction between the primary α-AlFeSi and β-Al_5FeSi phases. It may be suggested that direct imaging technique is a practical tool to analyze the detailed solidification behavior together with microstructural evolution.

References

[1] W. Eidhed: J. Mater. Sci. Tech. 24 (2008) 45-47.
[2] S. Murali, K. S. Raman and K. S. S. Murthy: Mater. Charact. 33 (1994) 99-112.
[3] P. Ashtari, H. Tezuka and T. Sato: Scr. Mater. 51 (2004) 43-46.
[4] P. Ashtari, H. Tezuka and T. Sato: Scr. Mater. 53 (2005) 937-942.